applied optics

Infrared sensitive liquid crystal light valve with semiconductor substrate

KONSTANTIN SHCHERBIN,[1,*] IGOR GVOZDOVSKYY,[1] AND DEAN R. EVANS[2]

[1]Institute of Physics, National Academy of Sciences, Prospekt Nauki 46, 03680 Kiev, Ukraine
[2]Air Force Research Laboratory, Materials and Manufacturing Directorate, Wright-Patterson Air Force Base, Ohio 45433, USA
*Corresponding author: kshcherb@iop.kiev.ua

Received 11 November 2015; revised 17 December 2015; accepted 11 January 2016; posted 11 January 2016 (Doc. ID 253761); published 9 February 2016

A liquid crystal light valve (LCLV) is an optically controlled spatial light modulator that allows recording of dynamic holograms. Almost all known LCLVs operate in the visible range of the spectrum. In the present work we demonstrate a LCLV operating in the infrared. The interaction of signal and pump waves is studied for different applied voltages, grating spacings, and intensities of the recording beams. A fourfold amplification of the weak signal beam is achieved. The amplitude of the refractive index modulation $\Delta n = 0.007$ and nonlinear coupling constant $n_2 = -1$ cm^2/W are estimated from the experimental results. External phase modulation of one of the recording beams is used for a further transient increase of the signal beam gain.

OCIS codes: (190.2055) Dynamic gratings; (070.6120) Spatial light modulators; (230.6120) Spatial light modulators; (260.3060) Infrared; (160.3710) Liquid crystals.

http://dx.doi.org/10.1364/AO.55.001076

1. INTRODUCTION

There is a need in nonlinear materials for dynamic gratings recording in the infrared spectral range because of possible application of these materials for information processing and transmission using available telecommunication components, which operate just in the infrared. Traditional photorefractive wide-bandgap ferroelectrics with large coupling constants in the visible spectral region generally are not at all sensitive in the infrared. There are only a few that are sensitive, such as rhodium-doped barium titanate [1] and tin hypothiodiphosphate [2], but these crystals usually are slow. Some photorefractive semiconductors, including gallium arsenide [3,4], indium phosphate [4], and cadmium telluride [5], are sensitive in the infrared, but moderate electro-optic coefficients usually result in relatively small coupling constants. In addition, the coupling constants are always reduced in the infrared as compared to the visible range of the spectrum because they are inversely proportional to the wavelength. Therefore, attaining a large coupling constant, which ensures large amplification of the weak beam, is not an easy task in the infrared.

One possible way to fulfill this task is combining in a single device a liquid crystal (LC) that usually exhibits huge birefringence and semiconductor sensitive in the infrared. In such hybrid devices, a driving force is created inside a photosensitive substrate. This driving force affects the LC and creates in it a spatial modulation of the refractive index with large amplitude. The dynamic hologram created in such a way in an LC may be used for signal processing in the infrared.

As far as we know, the first such organic–inorganic hybrid is the liquid crystal light valve (LCLV), which works in the reflection geometry. Devices of this type have been actively studied as spatial light modulators since the 1970s [6]. Later, the use of a transparent photoconductive substrate made from bulk crystalline $Bi_{12}SiO_{20}$ (BSO) allowed operation of an LCLV in the transmission geometry [7]. Recently, the nonlinear optical properties of LCLVs have been demonstrated in the near-infrared [8]. The recording of dynamic holograms was also reported [9] just after the present paper was submitted. In this work, we study an LCLV with a GaAs substrate, which allows recording of dynamic holograms in the infrared. The interaction of the recording waves is studied for different grating spacings, intensities, and intensity ratios of the recording beams. The nonlinear optical properties of the device are estimated from experimental data.

2. GAAS-BASED LCLV CELL AND EXPERIMENTAL SETUP

Figure 1(a) shows schematically the design of our LCLV cell. Optically finished 3-mm-thick 8 mm × 15 mm GaAs substrate serves as an input window. It is made of nominally undoped semi-insulating GaAs single crystal with dark resistivity of the order of 5×10^8 Ohm × cm. A relatively low absorption

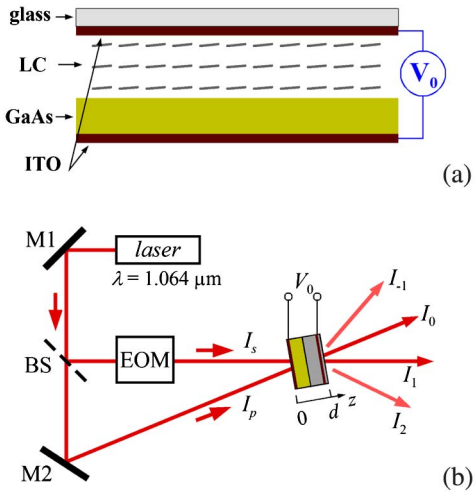

Fig. 1. Schematic representations of (a) the LCLV with GaAs substrate and (b) the experimental setup.

constant $\alpha \approx 1$ cm^{-1} at the wavelength $\lambda = 1.064$ μm results in only 25% reduction of the transmitted light intensity due to linear absorption. The Fresnel reflection losses are larger for GaAs with large refractive index $n = 3.5$, but they may be compensated by appropriate antireflection coating.

The transparent indium-tin oxide (ITO) electrode is deposited on the substrate from the outside face of the cell. The inside face of the output glass window is also coated with ITO electrode. The cell is filled by BL006 (Merck) LC. Spectral dependences of the ordinary and extraordinary refractive indices of this LC are known for the visible spectral range [10]. Extrapolation of the known data to $\lambda = 1.064$ μm allows us to estimate $n_o = 1.51$ and $n_e = 1.74$ for this wavelength. A mechanically rubbed polyimide alignment layer deposited on the inside face of the semiconductor substrate and on the glass face coated by ITO ensures planar orientation of the LC. The LC layer thickness $d = 10$ μm is set by spherical glass spacers. Sinusoidal ac voltage with amplitude $|V_0| \le 36$ V is applied to the ITO electrodes, ensuring that the electric field is applied across the substrate and liquid crystal.

The experimental setup is shown schematically in Fig. 1(b). The single-mode single-frequency diode-pumped Nd^{3+}:YAG laser emitting at 1.064 μm is used as a light source. The output laser radiation polarized in the plane of incidence is expanded and divided by a variable beam splitter (BS) into two beams, I_s and I_p, with typical intensity ratio $\beta = I_p(z = 0)/I_s(z = 0) \approx 80$. Both beams have a Gaussian intensity distribution with about 20 mm full width at half-maximum on the cell input face. A diaphragm with diameter 5 mm placed on the input cell face cuts the central part of the recording beams, ensuring spatial homogeneity of the light intensity within ±4%. The total light power is about 400 mW. Neutral density filters are used to change the light intensity. To separate the transmitted signal beam from the pump, its intensity is measured behind a 0.5-mm-diameter diaphragm placed at the focal plane of a lens with 25 cm focal length.

Two beams are crossed in the GaAs window, as shown in Fig. 1(b). The resulting interference pattern causes spatial modulation of the conductivity in the photoconductive GaAs substrate. This, in turn, results in corresponding spatial modulation of the voltage applied across the LC and, as a consequence, in spatial reorientation of the LC molecules. In this way, a refractive index grating is created in the LC layer. This grating may be used for processing of the infrared optical signals. A phase electro-optical modulator (EOM) is used in the experiments with external phase modulation.

3. WAVE MIXING IN THE GAAS-BASED LCLV: EXPERIMENTAL RESULTS AND DISCUSSION

A. Local Grating in LCLV for Amplification of the Weak Signal Beam

It is well known that the local index grating, i.e., the grating coinciding (or π shifted) with the interference pattern, cannot give rise to amplification of the signal beam in the steady state [11]. Obviously, the conductivity grating recorded in the photoconductive substrate is local. Therefore, amplification of the weak beam is not expected when using an LCLV. However, the grating recorded in the LCLV is not a typical local dynamic grating. Indeed, the index grating in the LC is rigidly attached to the conductivity grating created in the substrate. Thus, the grating in the LC is fixed thin local grating with respect to the recording interference fringes. Such a grating may give rise to the amplification of the weak beam thanks to diffraction of light from the strong pump beam in the direction of the weak signal. Understanding of this particular property of the LCLV allowed light beam amplification [12] in the visible spectral range.

To demonstrate signal beam gain with our LCLV, the temporal behavior of the transmitted weak signal beam is studied. A grating with spacing $\Lambda = 440$ μm is recorded by beams with total light intensity $I = 30$ mW/cm^2 and intensity ratio $\beta = 80$. The sinusoidal voltage with amplitude $V_0 = 2.6$ V and frequency $f = 20$ kHz is applied across the cell. The pump beam continuously illuminates the LCLV to keep electrical properties of the cell in the steady state. At time $t = 0$, the signal beam is unblocked. The temporal variation of the normalized intensity of the signal beam behind the cell $I_s(z = d, t)/I_s(z = 0, t)$ is shown in Fig. 2. The transmitted

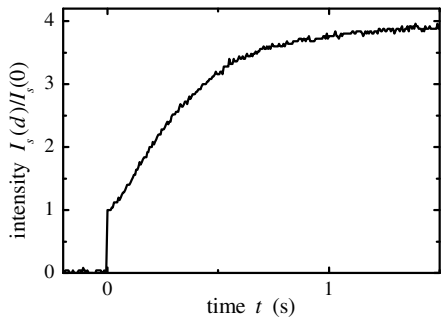

Fig. 2. Temporal dynamics of the transmitted signal beam measured for total light intensity $I = 30$ mW/cm^2, beam ratio $\beta = 80$, applied field with amplitude $V_0 = 2.6$ V, and frequency $f = 20$ kHz at grating spacing $\Lambda = 440$ μm. The pump beam continuously illuminates the LCLV, and the signal beam is unblocked at $t = 0$.

intensity increases with time, and fourfold gain $G = I_s(z = d)/I_s(z = 0) = 4$ is reached in the steady state. This gain is smaller than the gain $G = 10$ achieved with BSO-based LCLV in the visible spectral range [12], but larger than the largest gain $G = \exp(\Gamma d) = 2.7$ [13] ever achieved in a photorefractive semiconductor at $\lambda = 1.064$ μm without high voltage applied to the crystal. It should be noted that not much larger gain is achieved for $V_0 > 2.6$ V, but strong scattering makes difficult separation and intensity measurement of the transmitted beams for small intersection angles. That is why we limit the voltage to $V_0 = 2.6$ V in the experiments with large grating spacing (small intersection angles). The relatively low voltage results in relatively slow spatial reorientation of LC molecules and, correspondingly, in large grating formation time, which lies in the subsecond range $\tau \approx 350$ ms.

The grating in LC is thin and the LCLV operates in the Raman–Nath regime with the diffraction efficiency in the mth order defined as

$$\eta_m = J_m^2\left(\frac{\pi \Delta n d}{\lambda}\right), \tag{1}$$

where J_m is the Bessel function of the mth order and Δn is the amplitude of refractive index modulation in the LC layer. For large beam ratio $\beta \gg 1$, the diffraction efficiency is small ($\eta \ll 1$) and only the ± 1 orders of diffraction are important. The last fact is confirmed in the experiment—only ± 1 orders of diffraction are observed behind the LCLV. Therefore, the diffraction efficiency takes the form

$$\eta = \left(\frac{\pi \Delta n d}{\lambda}\right)^2. \tag{2}$$

Taking into account the diffraction from the pump, the intensity of the signal beam behind the cell may be written as

$$I_s(d) = I_s(0) + \eta I_p(0) = I_s(0) + \left(\frac{\pi \Delta n d}{\lambda}\right)^2 I_p(0). \tag{3}$$

The LCLV may be considered as a device exhibiting Kerr-like nonlinearity [12,14] with nonlinear coefficient $n_2 = \partial n/\partial I$, because the conductivity of the substrate (and therefore the voltage across the LC and the refractive index modulation) is linearly proportional to intensity in a certain intensity range. In this case, the amplitude of refractive index modulation is defined as $\Delta n = n_2 m I = 2 n_2 \sqrt{I_s I_p}$, where I is the total average light intensity and m is the contrast of the interference pattern. Thus, the gain of the signal beam may be written [12,14]

$$G = \frac{I_s(d)}{I_s(0)} = 1 + \left(\frac{2\pi n_2 I d}{\lambda}\right)^2, \tag{4}$$

where $I \approx I_p$ is the total light intensity.

By using Eq. (4), $|n_2| = 1$ cm$^2/W$ is estimated for $G = 4$ and $I = 30$ mW/cm^2. In spite of the fact that this value is smaller than the constant reported for an LCLV operating in the visible spectrum range [14], the estimated $|n_2|$ is so large that it ensures refractive index modulation $\Delta n \approx 0.007$ at our experimental conditions, as it is estimated using Eq. (3). It should be noted here that the constant n_2 is the characteristic of the cell in the present case, but it does not characterize a material as it is usually considered.

B. Determination of the Grating Shift

A self-defocusing is observed behind the cell for the incident beam with Gaussian intensity distribution. This observation shows that n_2 is negative, i.e., $n_2 = -1$ cm^2/W, as it is expected for $n_o < n_e$. To confirm this conclusion, we use the phase-modulation technique for determination of the grating phase shift [15]. The EOM introduces in the weak signal beam $I_s(0)$ a phase modulation $\Delta\phi \cos(2\pi f t)$ with a small amplitude $\Delta\phi = 0.12$ rad and fast frequency $f = 300$ Hz, which is much larger than the reciprocal relaxation time of the LCLV. This phase modulation, shown in Fig. 3(a), is transformed into intensity modulation behind the sample, as shown in Fig. 3(b). The intensity modulation is out-of-phase with respect to the input phase modulation with accuracy better than 0.01 rad. No intensity modulation with double frequency (second harmonic) is detected with the lock-in amplifier. Therefore, we conclude that the local π-shifted grating is recorded in the LCLV.

Indeed, the grating cannot follow small fast modulation, and, therefore, it is fixed with respect to the oscillating recording interference pattern. In the case of a local grating, any shift of the interference fringes results in the appearance of a nonlocal component of the grating. This nonlocal component gives unidirectional energy transfer, which is inherent to the nonlocal grating [11]. If the shift of the fringes in one direction gives amplification of the signal beam, the shift in the opposite direction gives attenuation, and vice versa. Therefore, the intensity modulation behind the grating at the frequency of the first harmonic of the input phase modulation unambiguously shows that the local grating is recorded [15] in our LCLV.

C. Optimization of Recording Conditions for Signal Beam Amplification

It is known from the first works on LCLVs [6,7] that the electrical properties of the cell are crucially important for its operation. The impedance of the substrate should be comparable with the impedance of the LC. Otherwise, light-induced changes in the substrate do not affect the LC. The LCLV circuit representation includes several resistor-capacitor circuits, which

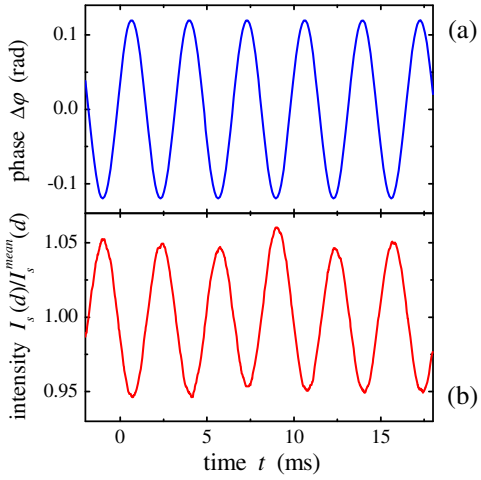

Fig. 3. (a) Phase modulation $\Delta\phi$ of the input signal beam $I_s(0)$ and (b) intensity modulation of this beam behind the crystal $I_s(d)$.

correspond to different layers of the cell [6,7]. That is why a resonance frequency exists that ensures optimal voltage across the LC layer for a certain voltage applied to the whole cell. At the same time, the electrical characteristics of different elements of the LCLV change with intensity change: (i) the resistance of the GaAs substrate changes because the substrate is photoconductive, and (ii) the capacitance of the LC changes because its dielectric permittivity changes when LC molecules are reoriented in the field. That is why the optimal frequency varies for different intensities. To find the optimal frequency for our cell, the dependence of the gain is measured as a function of frequency of the applied voltage for different intensities of the recording beams. The results are shown in Fig. 4 for $I = 8.5$ mW/cm^2 (circles), $I = 30$ mW/cm^2 (squares), and $I = 50$ mW/cm^2 (diamonds). The lines connect data measured at the same intensity. The resonant behavior of the gain on frequency is obvious. All experimental data are presented in this paper using the optimal frequencies.

The dependence of the gain as a function of intensity evaluated from the maxima of the curves like that shown in Fig. 4 is shown by the squares in Fig. 5. The line is plotted as a guide to the eye. The spatial modulation of the conductivity in the substrate becomes important when the photoconductivity

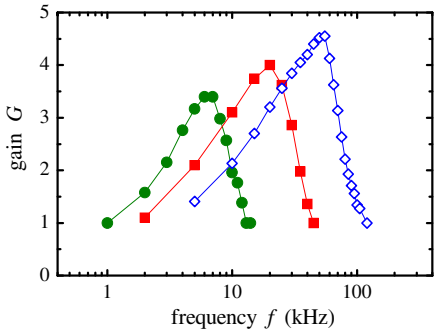

Fig. 4. Gain of the signal beam as a function of frequency of the applied voltage measured with voltage amplitude $V_0 = 2.6$ V at grating spacing $\Lambda = 440$ μm for total light intensity $I = 8.5$ mW/cm^2 (circles), $I = 30$ mW/cm^2 (squares), and $I = 50$ mW/cm^2 (open diamonds).

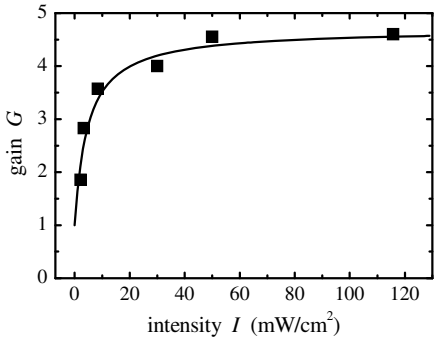

Fig. 5. Intensity dependence of the gain of the signal beam measured with voltage amplitude $V_0 = 2.6$ V at grating spacing $\Lambda = 440$ μm and at the optimal frequency for every intensity.

becomes larger than the dark conductivity. Correspondently, the gain rises while the intensity increases up to about 10 mW/cm^2. Then the gain is nearly constant in the wide range of intensity for which the conductivity of the substrate is comparable with the conductivity of the LC. One would expect for a large intensity that the gain would decrease because resistance of the substrate becomes small and does not affect the LC. We cannot reach such an intensity to confirm the last statement experimentally, because we have to use expanded beams.

To check the spatial resolution of the GaAs-based LCLV, we measure the gain as a function of grating spacing Λ. Experimental data are shown in Fig. 6. A gain, which can be reliably evaluated from the noise, is measured for $\Lambda > 90$ μm. This lower limit on fringe spacing is determined by the field spread in the substrate and LC [7]. The largest gain is measured at the largest possible grating spacing $\Lambda = 440$ μm. This upper limit on grating spacing is determined by overlapping of the transmitted beams behind the LCLV when the signal beam cannot be separated off the pump. The spatial resolution of the GaAs-based LCLV is relatively low, similar to other LCLVs operating in the visible [7]. However, the spatial resolution may be increased in the cell with optimized thickness of the substrate and LC layer, and a larger gain can be reached in such an optimized cell.

There is a technique that allows for a greater increase of the gain in the LCLV with an already optimized voltage, intensity, and grating spacing. It is known that step-like phase modulation of one of the recording beams by $\pi/2$ changes the grating from nonlocal to local and vice versa for a time interval smaller than the grating response time [16]. With such modulation, the interference pattern is translated by a quarter of a spatial period with respect to the recorded index grating, changing the type of response. We use this technique to increase gain in our LCLV. The grating is permanently recorded by beams with total light intensity $I = 30$ mW/cm^2 and beam ratio $\beta = 80$ at grating spacing $\lambda = 440$ μm. The fourfold gain is reached in the steady state. Then the phase of the signal beam is step-like modulated by $\pm\pi/2$, as shown in Fig. 7(a). The normalized output intensity of the signal beam is shown in Fig. 7(b). Just after the negative $\pi/2$ phase step, the eightfold transient gain is observed, which decreases smoothly to the steady-state gain $G \approx 4$ because the grating is rerecorded at a new position.

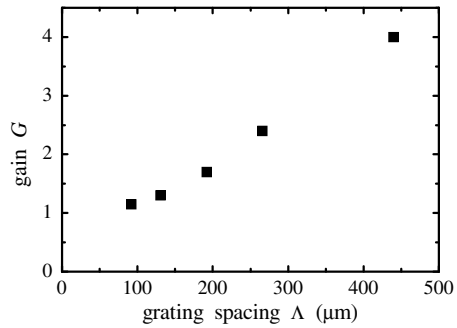

Fig. 6. Gain of the signal beam as a function of grating spacing measured with voltage amplitude $V_0 = 2.6$ V and total intensity $I = 30$ mW/cm^2.

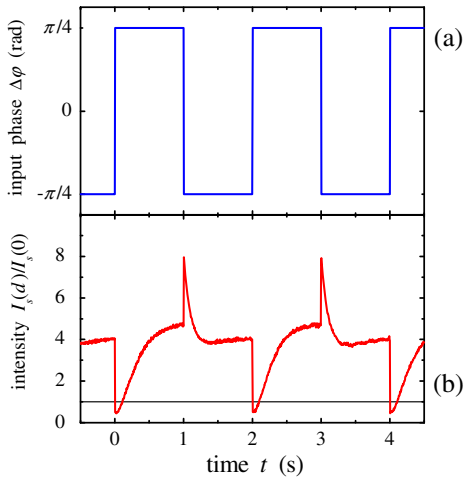

Fig. 7. (a) Step-like phase modulation $\Delta\phi(t)$ of the input signal beam $I_s(0)$ and (b) temporal dynamics of the normalized signal beam intensity behind the crystal $I_s(d, t)$.

The attenuation of the signal beam is observed with opposite phase step, as is expected, because the grating is translated in the opposite direction. The achieved transient gain can be used for processing of fast optical signals, as has been demonstrated with a CdTe-based adaptive interferometer [16].

D. Attenuation of the Signal Beam with High-Contrast Recording

Not only amplification, but sometimes attenuation, of the signal beam is used in applications. The attenuation of the signal can be achieved in the LCLV with high-contrast recording. Three higher orders of diffraction are observed behind our cell when the high-contrast grating is recorded by beams with nearly equal intensities. The appearance of these additional beams leads to considerable depletion of the pumps, one of which is the signal beam in this case. In such a way, attenuation of the recording beams may be achieved.

The temporal behavior of the transmitted signal is shown in Fig. 8. The grating is recorded by beams with intensity ratio close to unity $\beta \approx 1$ and total light intensity $I = 8.5$ mW/cm^2 at grating spacing $\Lambda = 440$ μm. The amplitude of applied voltage is $V_0 = 2.6$ V. Both beams are unblocked at time $t = 0$. The transmitted beam is depleted when grating recording starts, and more than 3 times attenuation of the signal beam is observed. This attenuation can be used for some applications, such as dynamic optical filters.

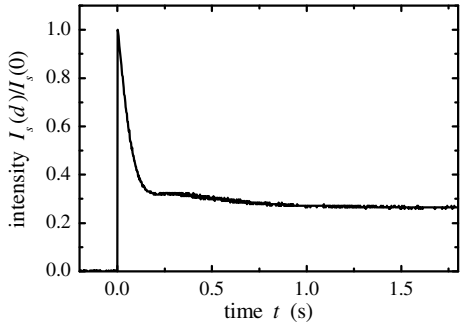

Fig. 8. Temporal dynamics of the transmitted signal beam measured for total light intensity $I = 8.5$ mW/cm^2, beam ratio $\beta = 1$, and applied field amplitude $V_0 = 2.6$ V at grating spacing $\Lambda = 440$ μm. Both recording beams are unblocked at $t = 0$.

4. CONCLUSIONS

Dynamic grating recording in the infrared is achieved in a GaAs-based LCLV. Fourfold gain of the weak signal beam is reached in the cell with properly selected GaAs substrate. This gain may be increased by using the technique of external phase modulation of the recording beams. For recording beams of equal intensity, more than 3 times attenuation of the signal beam may be achieved. Refractive index modulation $\Delta n = 0.007$ and nonlinear constant $n_2 = -1$ cm^2/W are estimated from the value of the gain $G = 4$ at total light intensity $I = 30$ mW/cm^2. It should be noted that the constant n_2 characterizes in the present case the LCLV as a whole, but not a material used in the LCLV. It is demonstrated that, out-of-phase, a local grating is recorded.

Funding. European Office of Aerospace Research and Development (118006); Science and Technology Center in Ukraine (P585)

REFERENCES

1. B. A. Wechsler, M. B. Klein, C. C. Nelson, and R. N. Schwartz, "Spectroscopic and photorefractive properties of infrared-sensitive rhodium-doped barium titanate," Opt. Lett. **19**, 536–538 (1994).
2. S. G. Odoulov, A. N. Shumelyuk, U. Hellwig, R. A. Rupp, and A. A. Grabar, "Photorefractive beam coupling in tin hypothiodiphosphate in the near infrared," Opt. Lett. **21**, 752–754 (1996).
3. M. B. Klein, "Beam coupling in undoped GaAs at 1.06 μm using the photorefractive effect," Opt. Lett. **9**, 350–352 (1984).
4. A. M. Glass, A. M. Jonson, D. H. Olson, W. Simpson, and A. A. Ballman, "Four-wave mixing in semi-insulating InP and GaAs using photorefractive effect," Appl. Phys. Lett. **44**, 948–950 (1984).
5. R. B. Bylsma, P. M. Bridenbaugh, D. H. Olson, and A. M. Glass, "Photorefractive properties of doped cadmium telluride," Appl. Phys. Lett. **51**, 889–891 (1987).
6. J. Grinberg, A. Jacobson, W. Bleha, L. Miller, L. Fraas, D. Boswell, and G. Myer, "A new real-time non-coherent to coherent light image converter–The hybrid field effect liquid crystal light valve," Opt. Eng. **14**, 143217 (1975).
7. P. Aubourg, J. P. Huignard, M. Hareng, and R. A. Mullen, "Liquid crystal light valve using bulk monocrystalline $Bi_{12}SiO_{20}$ as the photoconductive material," Appl. Opt. **21**, 3706–3712 (1982).
8. U. Bortolozzo, S. Residori, and J. P. Huignard, "Transmissive liquid crystal light-valve for near-infrared applications," Appl. Opt. **52**, E73–E77 (2013).
9. A. Peigné, U. Bortolozzo, S. Residori, S. Molin, P. Nouchi, D. Dolfi, and J. P. Huignard, "Adaptive holographic interferometer at 1.55 μm based on optically addressed spatial light modulator," Opt. Lett. **40**, 5482–5485 (2015).
10. J. Li, G. Baird, Y. H. Lin, H. Ren, and S. T. Wu, "Refractive index matching between liquid crystals and photopolymers," J. Soc. Inf. Display **13**, 1017–1026 (2005).
11. N. V. Kukhtarev, V. B. Markov, S. G. Odoulov, M. S. Soskin, and V. L. Vinetskii, "Holographic storage in electrooptic crystals. I. Steady state," Ferroelectrics **22**, 949–960 (1978).
12. A. Brignon, I. Bongrand, B. Loiseaux, and J. P. Huignard, "Signal-beam amplification by two-wave mixing in a liquid-crystal light valve," Opt. Lett. **22**, 1855–1857 (1997).

13. K. Shcherbin, "High photorefractive gain at counterpropagating geometry in CdTe:Ge at 1.064 μm and 1.55 μm," Appl. Opt. **48**, 371–374 (2009).
14. U. Bortolozzo, S. Residori, and J. P. Huignard, "Beam coupling in photorefractive liquid crystal light valves," J. Phys. D **41**, 224007 (2008).
15. P. M. Garcia, L. Cescato, and J. Frejlich, "Phase-shift measurement in photorefractive holographic recording," J. Appl. Phys. **66**, 47–49 (1989).
16. K. Shcherbin and M. B. Klein, "Adaptive interferometers with no external field using reflection gratings in CdTe:Ge at 1550 nm," Opt. Commun. **282**, 2580–2585 (2009).